Reactive Oxygen Species Regulate Activity-Dependent Neuronal Structural Plasticity

Matthew C. W. Oswald[1], Paul S. Brooks[1], Maarten F. Zwart[2], Amrita Mukherjee[1], Ryan J. H. West[3], Khomgrit Morarach[1], Sean T. Sweeney[3*], Matthias Landgraf[1*]

[1] University of Cambridge, Department of Zoology, Downing Street, Cambridge, CB2 3EJ, United Kingdom

[2] HHMI Janelia Research Campus, Ashburn, VA, 20147, USA

[3] Department of Biology, University of York, Heslington York YO10 5DD, United Kingdom

* corresponding authors: sean.sweeney@york.ac.uk ml10006@cam.ac.uk

Neurons adjust their excitability, connectivity and structure in response to changes in activity, yet how neurons sense their activity level remains unclear. We have found that motorneurons cell-autonomously monitor their activity by responding to the levels of reactive oxygen species (ROS), a metabolic mitochondrial byproduct. The highly conserved Parkinson's disease-linked protein DJ1b is central to this, acting as a redox sensor to regulate pre- and postsynaptic structural plasticity via activation of the PI3Kinase pathway.

Plasticity is fundamental to neuronal development and function. Neurons respond to changes in activity regimes by adjusting their intrinsic excitability and the structure and efficacy of synapses. Such adjustments can be compensatory, working toward maintaining neuronal or network activity within a set range. Alternatively, associative input-specific Hebbian plasticity results in local changes to synaptic strength[1].

We set out to study how neurons measure changes in activity and which cellular mechanisms mediate activity-regulated structural adjustments, focusing on two identified motorneurons ('aCC' and 'RP2') in the *Drosophila* larva. At presynaptic neuromuscular junction (NMJ) terminals temperature stimulated increases in locomotor activity (e.g. raise to 29 °C) lead to addition of boutons (varicosities containing active zones)[2]. We find similar presynaptic structural adjustments result from cell-autonomous increases in neuronal activity via targeted expression of the warmth gated ion channel dTrpA1, bouton number scaling with neural activity[3] (**Fig. 1a** and **c**). In contrast, the size of motorneuron postsynaptic dendritic arbors in the

central nervous system (CNS) negatively correlates with neural activity (**Fig. 1b** and **d**). Since aCC motorneurons reduce dendritic growth when over-innervated and *vice versa*[4] , and arbor size regulates input synapse number and thus synaptic drive[5], we interpret this as a homeostatic adjustment.

We next asked what signals might neurons use to gauge activity levels. Many studies have implicated calcium as an important signal[1]. In view of the energetic cost of neural activity[6], we wondered whether neurons might also measure activity levels metabolically. We focused on ROS, the superoxide anion (O_2-), and hydrogen peroxide (H_2O_2), as these are obligate byproducts of mitochondrial respiratory ATP synthesis. Though intensively studied as destructive agents when at high concentration in the context of ageing and neurodegenerative conditions, in healthy cells ROS are necessary for many physiological processes, including growth factor signalling[7]. In the nervous system, ROS regulate NMJ growth in *Drosophila*[8], and in vertebrates ROS have been implicated in activity-dependent Hebbian plasticity[9]. Indeed, we find that highly active neurons produce more ROS as indicated by a mitochondrion-targeted ratiometric ROS reporter (mito-roGFP2-Orp1)[10] (**Supplementary Fig. 1**). We therefore hypothesised that metabolic ROS might provide a read-out of neuronal activity and regulate synaptic structural plasticity. To test this hypothesis, we first cell-autonomously increased neuronal activity while over-expressing the ROS scavenging enzymes Superoxide Dismutase 2 (SOD2, which catalyses O_2- to H_2O_2 conversion) or Catalase (H_2O_2 into H_2O). Catalase co-expression significantly counteracts dTrpA1-induced bouton addition at the NMJ (**Fig. 2a**) and rescues dendritic size in the CNS (**Fig. 2b**). SOD2 co-expression on the other hand enhances dTrpA1-mediated NMJ elaboration, presumably because of potentiated H_2O_2 production (**Fig. 2a**). We then confirmed that ROS are sufficient to invoke structural plasticity when applied systemically, via paraquat or Di-ethylmaleate (DEM)[8], or induced cell-autonomously within motorneurons by knockdown of ROS scavengers or Dual oxidase expression (**Fig. 2c**). Thus, we implicate ROS, specifically H_2O_2, in activity-dependent structural plasticity.

We identified *DJ1b*, the fly ortholog of DJ1, as a candidate ROS sensor. *DJ1*, first isolated in 1997[11], is a highly conserved, ubiquitously expressed gene whose protein product is redox-sensitive, protecting against oxidative stress and regulating mitochondria[12]; a mutant allele is also linked to a rare form of familial Parkinsonism[13]. In flies, *DJ1b* null mutant (*DJ1b*$^{\Delta 93}$) larvae[14] develop normally and have structurally

normal NMJs (**Supplementary Fig. 2**), but these are significantly less sensitive to both systemic and cell-autonomous ROS (**Fig. 3a**). Compellingly, both systemic loss of *DJ1b* and motorneuron-specific expression of a dominant acting mutant form of DJ1b, non-oxidisable at conserved cysteine 104 (*DJ1bC104A*) rescue dTrpA1 activity-mediated NMJ phenotypes (**Fig. 3a**). Likewise, in $DJ1b^{\Delta 93}$ mutant larvae, temperature (29 ^{o}C) stimulated increase in locomotor activity fails to produce presynaptic bouton addition (**Fig. 3b**). At the postsynaptic dendritic arbor, removal of one copy of *DJ1b* ($DJ1b^{\Delta 93/+}$) is sufficient to significantly suppress dTrpA1-mediated reductions in arbor length (**Supplementary. Fig. 3**). These data show that DJ1b is necessary for ROS sensing and structural plasticity in response to increased neuronal activity.

DJ1 is a known redox-regulated inhibitor of Phosphatase and Tensin homologue (PTEN) and negative regulator of the PI3Kinase pathway[15,16]; PI3Kinase is a positive regulator of NMJ development[17]. To test whether DJ1b - PTEN interactions mediate ROS dependent NMJ adjustments, we performed genetic epistasis experiments in the context of a DEM dose-response gradient (**Fig. 3c**). Deletion of one copy of *DJ1b* ($DJ1b^{\Delta 93/+}$) suppresses DEM-induced NMJ elaboration. In contrast, $PTEN^{CO76/+}$ heterozygous larvae show increased sensitivity to DEM. Larvae trans-heterozygous for both *DJ1b* and *PTEN* ($PTEN^{CO76/+}$; $DJ1b^{\Delta 93/+}$) are less sensitive to DEM compared to $PTEN^{CO76/+}$ larvae. These data complement previous biochemical data[15,16] and suggest that DJ1b negatively regulates PTEN to mediate ROS-induced structural plasticity.

We then manipulated PTEN and PI3Kinase activities cell-autonomously. Targeted knock-down of PTEN sensitises motorneurons to ROS. In contrast, over-expression of PTEN or mis-expression of a dominant negative form of PI3Kinase ($PI3K^{DN}$) significantly rescue the NMJ elaboration phenotypes caused by DEM exposure or dTrpA1-mediated increased neuronal activity, suggesting that PTEN and PI3Kinase act downstream of DJ1 and neural activity generated ROS (**Fig. 3d**).

In conclusion, we have identified a pathway by which neurons sense changes in activity and translate these into structural changes at pre- and postsynaptic terminals. We show ROS, byproducts of mitochondrial respiration, are necessary and sufficient second messengers, suggesting that neurons respond to activity-induced changes in metabolic rate. We propose that DJ1b, acting as a redox sensor,

activates PI3Kinase signalling via redox-regulated inhibition of PTEN (**Fig. 3e**), well-known intermediates of metabolic signalling pathways and synaptic feedback mechanisms[18]. Building on this study we can now determine how these structural adjustments impact on synaptic connectivity, and whether this ROS-DJ1b-PI3Kinase pathway also co-ordinates regulation of neuronal excitable properties.

AUTHOR CONTRIBUTIONS

M.O., S.T.S. & M.L. devised the project. M.O. performed most experiments and analyses. P.B., A.M., M.F.Z. & K.M. generated specimens and dendrite data on activity dependent dendrite growth. A.M. carried out experiments and analysis involving ROS measurements. R.J.H.W. processed specimens for TEM imaging and analysed TEM data.

M.O. & M.L. co-wrote the manuscript and S.T.S. & M.L. co-supervised the project.

Acknowledgements:

We would like to thank Nancy Bonini, Tobias Dick, Jörg Grosshans, Karen Hibbard, Fanis Missirlis, Barret Pfeiffer and Alex Whitworth for generous reagent donations. We would also like to thank Jimena Berni, Alex Whitworth and members of the Landgraf lab for valuable comments on the manuscript. This work was supported by BBSRC research grants (BB/IO1179X/1, BB/M002934/1) to ML and (BB/I012273/1, BB/M002322/1) to STS.

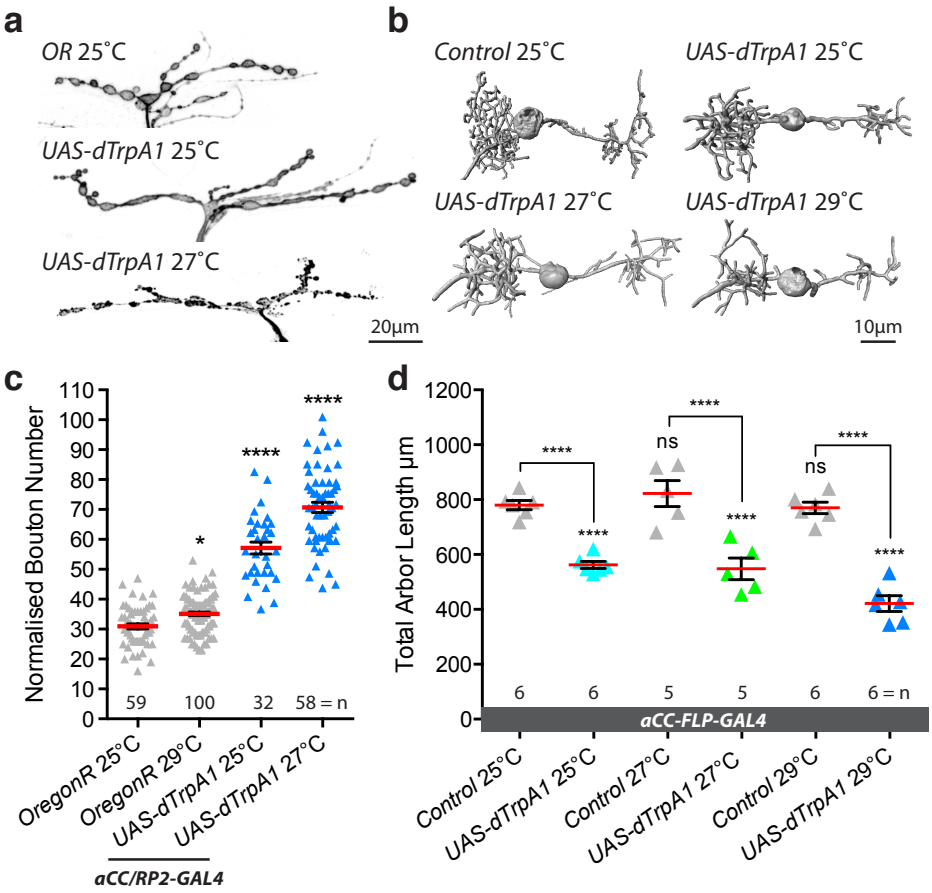

Figure 1: Motorneurons structurally adjust input and output terminals in response to increased activity. Representative images (**a**) and bouton number dot plot quantification (**c**) of presynaptic wandering 3rd instar NMJs showing titratable behaviourally and cell-autonomously-induced activity-dependent elaboration. 'aCC/RP2-GAL4' expresses in all larval aCC and RP2 motorneurons (see **Online Methods**). Digital reconstructions (**b**) and total arbor length dot plots (**d**) showing 24hr ALH (after larval hatching) aCC neuron post-synaptic arbors (input) display activity-dependent reduced arbor length. 'aCC-FLP-GAL4' used to manipulate single aCC neurons (see **Online Methods**), 'Control' is aCC-FLP-GAL4 alone. Mean +/- SEM, ANOVA, ns = not significant P>0.05, *P<0.05, ****P<0.0001, n = replicate number.

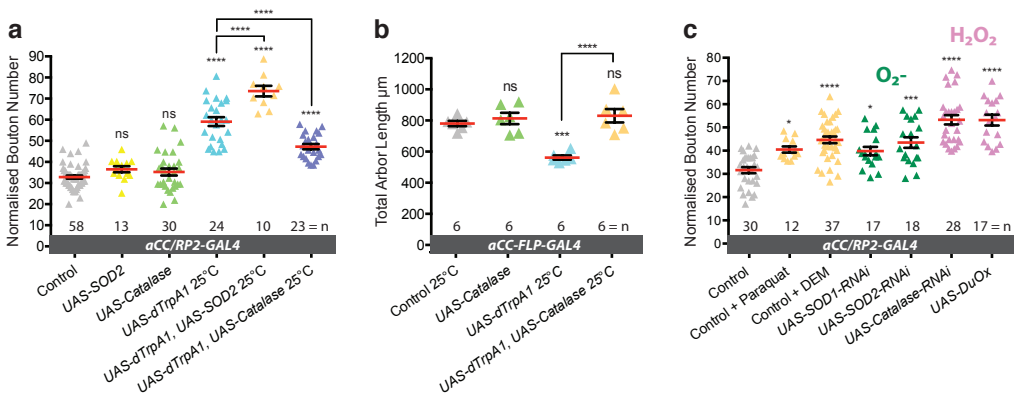

Figure 2: ROS are necessary and sufficient for activity-dependent structural plasticity. (**a**) Bouton number dot plots showing that co-expression of UAS-SOD2 exacerbates while that of UAS-Catalase rescues UAS-dTrpA1-mediated structural adjustment (wandering 3rd instar, aCC/RP2-GAL4, 'Control' is aCC/RP2-GAL4 alone) (**b**) Total dendritic arbor length dot plots showing UAS-Catalase co-expression significantly rescues activity-driven arbor length reduction (24hr ALH larvae, aCC-FLP-GAL4, 'Control' is aCC-FLP-GAL4 alone). (**c**) Bouton number dot plots showing that systemic and cell-autonomous ROS elevations are sufficient to induce NMJ elaboration (wandering 3rd instar, aCC/RP2-GAL4, 'Control' is aCC/RP2-GAL4 alone). Mean +/- SEM, ANOVA, ns = not significant P>0.05, *P<0.05, ***P<0.001, ****P<0.0001, n = replicate number.

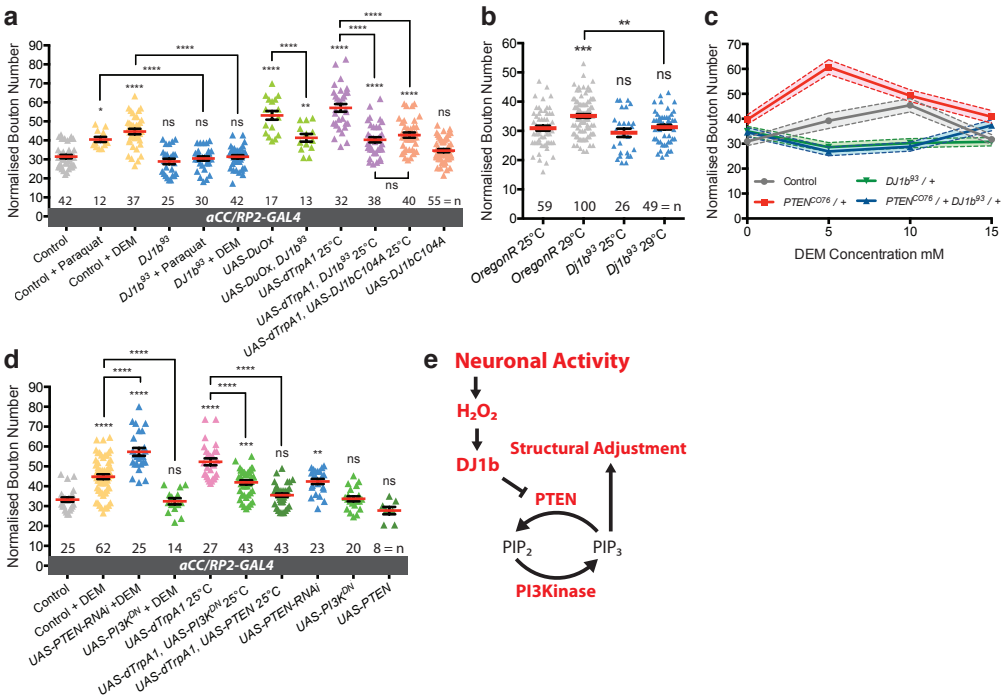

Figure 3: ROS signal via DJ1b, PTEN and PI3Kinase to regulate activity-dependent structural plasticity. (**a**) Systemic ROS, cell-autonomous ROS and activity-induced NMJ structural adjustments require DJ1b. (**b**) DJ1b is required for 29 °C-induced NMJ elaboration. (**c**) DJ1b and PTEN genetically interact to regulate systemic ROS-induced NMJ elaboration. Dashed boundary indicates 95 % confidence interval (n≥38). (**d**) Systemic ROS and activity-induced NMJ structural adjustments require PTEN and PI3Kinase signalling. (**e**) Model summary: neuronal activity-induced ROS oxidise DJ1b, promoting binding to and inhibition of PTEN, thus releasing inhibition upon PI3Kinase signalling. Bouton number dot plots from wandering 3rd instar larval NMJs, using aCC/RP2-GAL4 where indicated, 'Control' is aCC/RP2-GAL4 alone. Mean +/- SEM, ANOVA, ns = not significant P>0.05, *P<0.05, **P<0.01, ***P<0.001, ****P<0.0001, n = replicate number.

References

1. Turrigiano, G. *et al. Cold Spring Harb. Perspect. Biol.* **4**, a005736 (2012)
2. Sigrist, S.J. *et al. J. Neurosci.* **23**, 6546-6556 (2003)
3. Pulver, S. R. *J. Neurophysiol.* **101**, 3075–3088 (2009)
4. Tripodi, M. *et al. PLoS Biol.* **6**, 2172-2187 (2008)
5. Zwart, M. *et al. PNAS* **110**, 3878-3887 (2013)
6. Attwell, D. and Laughlin, S. B. *J. Cereb. Blood Flow Metab.* **21**, 1133-1145 (2001)
7. Finkel, T. *et al. J. Cell Biol.* **194**, 7-15 (2011)
8. Milton, V. *et al. Proc. Natl. Acad. Sci. U.S.A.* **108**, 17521-17526 (2011)
9. Hongpaisan, J. *et al. J. Neurosci.* **24**, 10878-10887 (2004)
10. Gutscher, M. *et al. J. Biol. Chem.* **284**, 31532-31540 (2009)
11. Nagakubo, D. *et al. Biochem. Biophys. Res. Commun.* **231**, 509-513 (1997)
12. Ariga, H. *et al. Oxid. Med. Cell. Longev.* **2013**, 9 pages (2013)
13. Bonifati, V. *et al. Science* **299**, 256-259 (2002)
14. Meulener, M. C. *et al. Curr. Biol.* **15**, 1572-1577 (2005)
15. Kim, R. H. *et al. Cancer Cell* **7**, 263-273 (2005)
16. Kim, Y. *et al. Int. J. Oncol.* **35**, 1331-1341 (2009)
17. Martín-Peña, A. *et al. J. Neurosci.* **26**, 10199–10208 (2006)
18. Howlett, E. *et al. PLoS Genet.* **4**, e10000277 (2008)

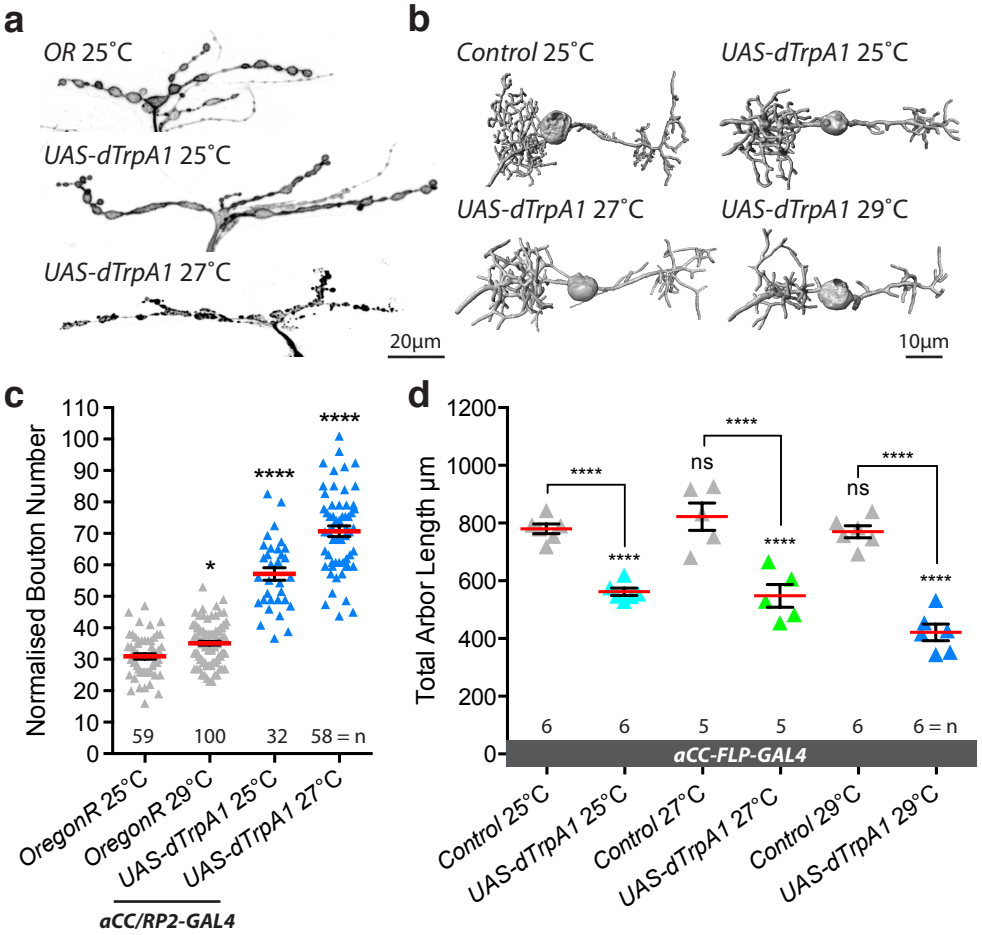
a
OR 25˚C
UAS-dTrpA1 25˚C
UAS-dTrpA1 27˚C
20µm
b
Control 25˚C
UAS-dTrpA1 25˚C
UAS-dTrpA1 27˚C
UAS-dTrpA1 29˚C
10µm
c
Normalised Bouton Number
110
100
90
80
70
60
50
40
30
20
10
0
59
100
32
58 = n
*
****
****
OregonR 25°C
OregonR 29°C
UAS-dTrpA1 25°C
UAS-dTrpA1 27°C
aCC/RP2-GAL4
d
Total Arbor Length µm
1200
1000
800
600
400
200
0
****
****
ns
****
****
ns
****
6
6
5
5
6
6 = n
aCC-FLP-GAL4
Control 25°C
UAS-dTrpA1 25°C
Control 27°C
UAS-dTrpA1 27°C
Control 29°C
UAS-dTrpA1 29°C

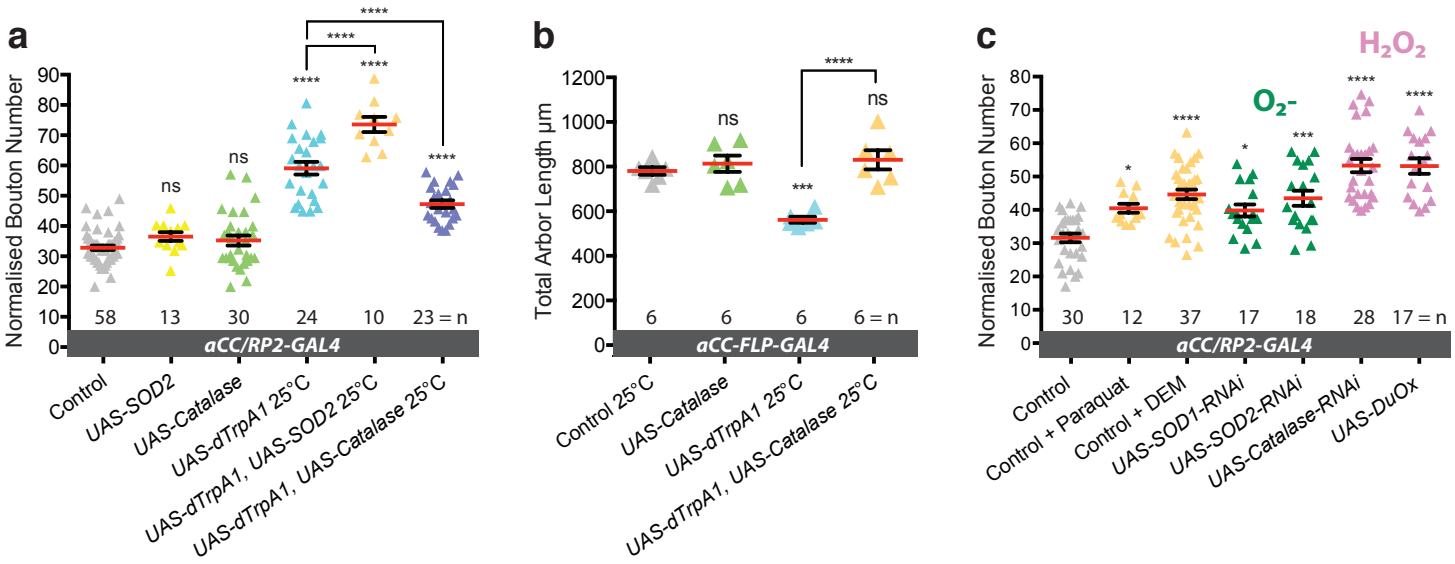
a
Normalised Bouton Number
90
80
70
60
50
40
30
20
10
0
****
****
****
****
ns
ns
58
13
30
24
10
23 = n
aCC/RP2-GAL4
Control
UAS-SOD2
UAS-Catalase
UAS-dTrpA1 25°C
UAS-dTrpA1, UAS-SOD2 25°C
UAS-dTrpA1, UAS-Catalase 25°C
b
Total Arbor Length µm
1200
1000
800
600
400
200
0
****
ns
ns
***
6
6
6
6 = n
aCC-FLP-GAL4
Control 25°C
UAS-Catalase
UAS-dTrpA1 25°C
UAS-dTrpA1, UAS-Catalase 25°C
c
Normalised Bouton Number
80
70
60
50
40
30
20
10
0
H2O2
O2-
*
****
*
***
****
****
30
12
37
17
18
28
17 = n
aCC/RP2-GAL4
Control
Control + Paraquat
Control + DEM
UAS-SOD1-RNAi
UAS-SOD2-RNAi
UAS-Catalase-RNAi
UAS-DuOx

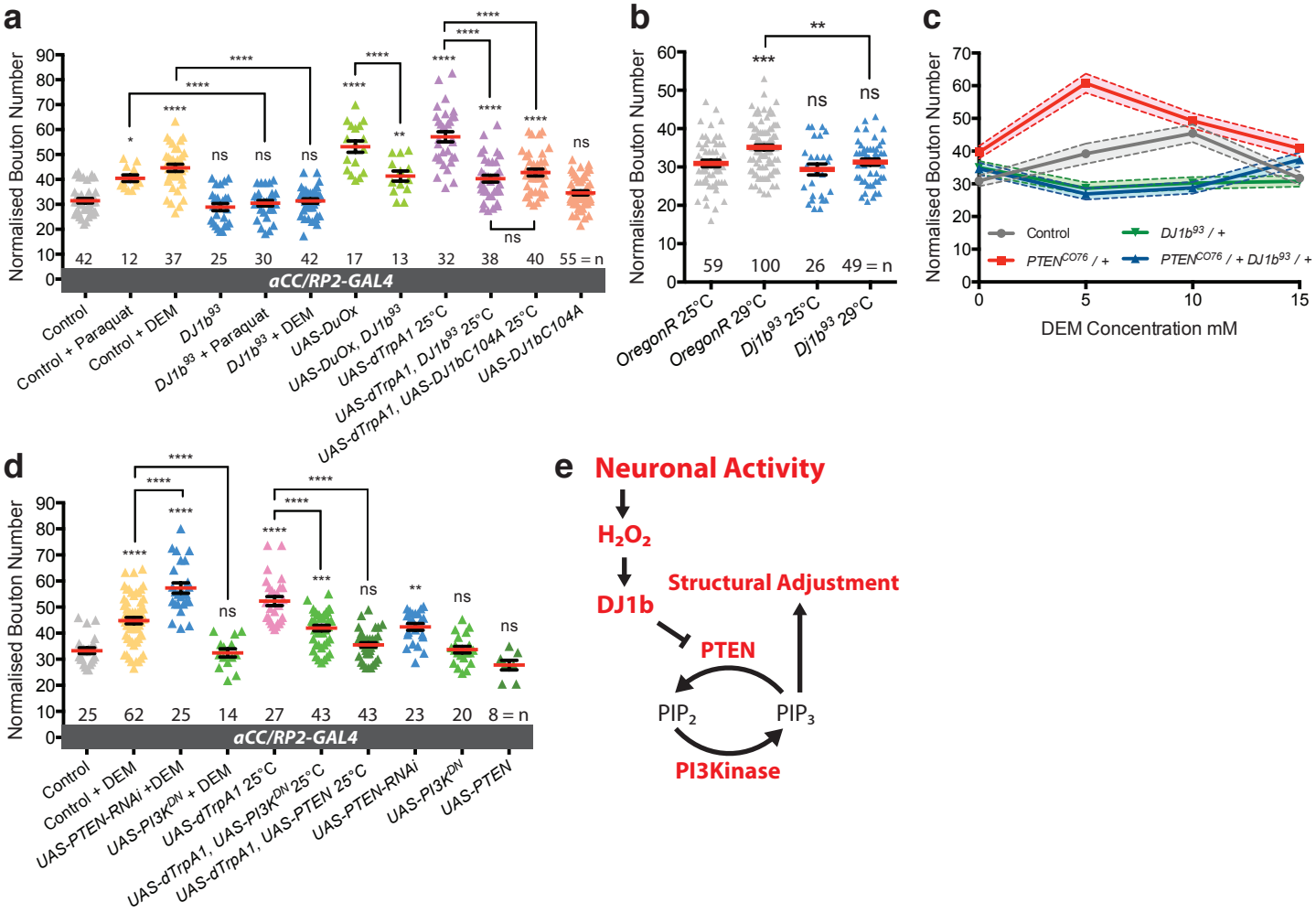
a
Normalised Bouton Number
aCC/RP2-GAL4
Control
Control + Paraquat
Control + DEM
DJ1b93
DJ1b93 + Paraquat
DJ1b93 + DEM
UAS-DuOx
UAS-DuOx, DJ1b93
UAS-dTrpA1 25°C
UAS-dTrpA1, DJ1b93 25°C
UAS-dTrpA1, UAS-DJ1bC104A 25°C
UAS-dTrpA1, UAS-DJ1bC104A
42 12 37 25 30 42 17 13 32 38 40 55 = n
b
Normalised Bouton Number
OregonR 25°C
OregonR 29°C
Dj1b93 25°C
Dj1b93 29°C
59 100 26 49 = n
c
Normalised Bouton Number
DEM Concentration mM
Control
DJ1b93 / +
PTENCO76 / +
PTENCO76 / + DJ1b93 / +
d
Normalised Bouton Number
aCC/RP2-GAL4
Control
Control + DEM
UAS-PTEN-RNAi +DEM
UAS-PI3KDN + DEM
UAS-dTrpA1 25°C
UAS-dTrpA1, UAS-PI3KDN 25°C
UAS-dTrpA1, UAS-PTEN 25°C
UAS-PTEN-RNAi
UAS-PI3KDN
UAS-PTEN
25 62 25 14 27 43 43 23 20 8 = n
e
Neuronal Activity
H2O2
DJ1b
Structural Adjustment
PTEN
PIP2
PIP3
PI3Kinase